Distance-redshift relation in an isotropic inhomogeneous universe: Spherically symmetric dust-shell universe

Norimasa Sugiura,* Ken-ichi Nakao,† and Tomohiro Harada‡
Department of Physics, Kyoto University, Sakyo-ku, Kyoto 606-8502, Japan
(Received 26 May 1998; published 8 October 1998)

The relation between the angular diameter distance and redshift (d_A-z relation) in a spherically symmetric dust-shell universe is studied. This model has large inhomogeneities of matter distribution on small scales. We have discovered that the relation agrees with that of an appropriate Friedmann-Lemaître (FL) model if we set a ''homogeneous'' expansion law and a ''homogeneous'' averaged density field. This will support the averaging hypothesis that a universe looks like a FL model in spite of small-scale fluctuations of density field, if its averaged density field is homogeneous on large scales. [S0556-2821(98)09320-5]

PACS number(s): 98.80.Es, 04.30.Nk, 04.50.+h, 95.30.Sf

I. INTRODUCTION

The standard big bang model is based on the assumption of the homogeneous and isotropic distribution of matter and radiation. This assumption then leads to the Robertson-Walker (RW) space-time geometry and the Friedmann-Lemaître (FL) universe model[1] through the Einstein equations. This model has succeeded in explaining various important observational facts: Hubble's expansion law, the content of light elements and the isotropy of the cosmic microwave background radiation (CMBR) [1].

The CMBR conversely gives a strong observational basis for the assumption of homogeneity and isotropy of our universe by its highly isotropic distribution together with the Copernican principle. Indeed, the deviation of our universe from a homogeneous and isotropic space is as small as 10^{-5} [2] at the stage of decoupling. Thus our universe is well approximated by a FL model before this stage. On the other hand, the present universe is highly inhomogeneous on small scales; the density contrast is of the order of 10^{30} in the solar system, 10^5 on galactic scales, and of the order of unity even on the scale of superclusters. We have to go beyond FL models in considering such systems.

For a long time, we have regarded that a FL model is a large-scale ''average'' of a locally inhomogeneous universe (averaging hypothesis). Even though the observational data are consistent with the picture that our universe is described well by a RW metric, we are not sure how to derive the background FL model from the inhomogeneous universe by any averaging procedure, or how the non-linear inhomogeneities on small scales affect large-scale behavior of the universe [3]. Although one can derive a background FL model from observations of the nearby galaxies with any rule of averaging one likes, it is uncertain whether this background FL model agrees with the FL model whose cosmological parameters were defined at the stage of decoupling. The discrepancies might appear, for example, in the estimate of the density of baryonic matter, the density parameter, the age of our universe, and so on. These still remain a non-trivial question to which we have to give a clear answer.

A number of approaches have been made to study how the small-scale inhomogeneities affect the global dynamics when averaged on larger scales [4–7]. The first work which explicitly showed the existence of such an effect was performed by Futamase [4]. Assuming small deviation of the space-time geometry from the RW one, Futamase constructed an elegant formalism by the use of the post-Newtonian expansion and Isaacson's prescription to take into account the back reaction of the small-scale inhomogeneities on the global cosmic expansion. After his works, Buchert and Ehlers [5] studied this back reaction problem in the framework of the Newtonian cosmology in which the corresponding background FL model is uniquely determined through the spatial averaging of physical quantities without any uncontrolled approximation. They showed that inhomogeneities do not influence the overall expansion in spatially compact models (the topology of its spatial section is T^3) if they are averaged over the whole space. In other cases, the significance of inhomogeneities may depend on the cosmology one adopts. Another interesting approach has been made by Carfora and Piotrkowska [7], in which three-dimensional geometry is deformed according to the Ricci-Hamiltonian flow which they say would be equivalent to changing the scale of averaging. They derive a homogeneous geometry which corresponds to a large-scale average of an inhomogeneous universe, and discussed the effect of inhomogeneities on the cosmological parameters.

In spite of these works, the effect of inhomogeneities on the cosmological parameters remains unclear; there are even apparent discrepancies in their statements. The reason seems to lie in the different definition of back reaction of inhomogeneities [8]; its definition is ambiguous since they do not treat observable quantities in these works. Thus, in order to understand clearly the effects of inhomogeneities, it is necessary to relate them with physical quantities which we can give an unambiguous definition.

*Email address: sugiura@tap.scphys.kyoto-u.ac.jp
†Email address: nakao@tap.scphys.kyoto-u.ac.jp
‡Email address: harada@tap.scphys.kyoto-u.ac.jp

[1]We use the term ''Robertson-Walker space-time'' when we focus on geometrical aspects of a homogeneous and isotropic model, and ''Friedmann-Lemaître model'' when we discuss its dynamics and observable quantities.

Bildhauer [9] showed that the global cosmic expansion rate is not isotropic if the back reaction of small-scale inhomogeneities are taken into account and then investigated its observational effects on the CMBR. After this work, Bildhauer and Futamase [10] discussed the possibility that the observed dipole anisotropy in the CMBR comes from this effect. These works are significant in the sense that the back reactions on the observable quantities were discussed, but they did not consider the cases where we try to determine the cosmological parameters by observing an inhomogeneous universe.

In this paper, we investigate the relation between distance and redshift in an inhomogeneous universe. As an inhomogeneous model, we take a spherically symmetric dust-shell model, in which light rays travel from each dust shell toward an observer at the center. We calculate angular diameter distance-redshift (d_A-z) relation and compare it with that of a FL model. Our main goal in this paper is to clarify the condition under which the distance-redshift relation of a dust-shell universe behaves like that of a FL model. We investigate the behavior of the averaged density around the observer at the center when we gradually extend the averaged region to the outer shells, and discuss the relation among the behavior of the averaged density, the energy density of the FL model, and the observed distance-redshift relation.

We note two interesting points of a dust-shell model. First, its dynamics is exactly solved; it is not necessary to assume the existence of homogeneous background in order to obtain the behavior of density fluctuations. Secondly, it can treat a discrete mass distribution where the linear perturbation theory is invalid, and can also treat a highly general-relativistic situation where the scale of inhomogeneities are comparable to the horizon scale.

The organization of this paper is as follows. In the next section, we present basic equations for the dynamics of a dust-shell universe, distance to the shells from the center, and redshift of the shells measured by an observer at the center. We give our results and discussion on d_A-z relation and averaged density in Sec. III, followed by concluding remarks in Sec. IV.

We follow the sign convention of the Riemann tensor and the metric tensor in [11] and adopt the unit of $c=1$.

II. FORMULATION OF DUST-SHELL UNIVERSE

A. Equation of motion of dust-shell

We put a number of spherically symmetric shells whose centers are common at $r=0$ (see Fig. 1). The innermost shell is called the first shell, the next one is called the second shell, and so on. The region enclosed by the $(i-1)$th shell and ith shell is called the ith region. Each shell is infinitesimally thin, characterized by the surface stress-energy tensor which is given by

$$S^{ab} \equiv \lim_{\epsilon \to 0} \int_{-\epsilon}^{+\epsilon} T^{ab} dx, \tag{2.1}$$

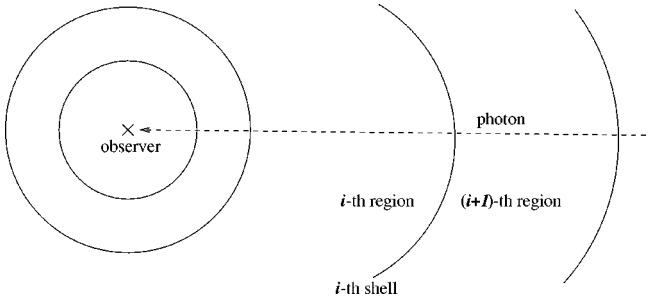

FIG. 1. Dust-shell universe.

where x is a Gaussian coordinate ($x=0$ on the shell) in the direction normal to the shell.

Since each region between the shells is vacuum, the space-time is described by the Schwarzschild geometry by the Birkhoff's theorem. The line element in the ith region is written in the form

$$ds_i^2 = -\left(1-\frac{2Gm_i}{r}\right)dt^2 + \left(1-\frac{2Gm_i}{r}\right)^{-1} dr^2 + r^2 d\Omega^2, \tag{2.2}$$

where the parameter m_i will be referred to as a gravitational mass ($m_1=0$), and $d\Omega$ is the line element of a unit sphere.

We first derive the expansion law of the ith shell following [12–15]. Let n^a be a unit space-like vector normal to the trajectory of the shell, and define the projection operator $h_a^b \equiv \delta_a^b - n_a n^b$. From the projected Einstein equation

$$R_{ab}h_c^a h_d^b = 8\pi G\left(T_{ab} - \frac{1}{2}g_{ab}T\right)h_c^a h_d^b, \tag{2.3}$$

one obtains

$$\pounds_n K_{cd} + {}^3R_{cd} - KK_{cd} = 8\pi G\left(T_{ab}h_c^a h_d^b - \frac{1}{2}h_{cd}T\right), \tag{2.4}$$

where $\pounds_n$ is the Lie derivative along n^a and ${}^3R_{cd}$ is the three-dimensional Ricci tensor on the timelike hypersurface generated by the motion of the shell. The extrinsic curvature K_{ab} is defined by $K_{ab} = -\frac{1}{2}h_a^c h_b^d \pounds_n h_{cd}$, and $K = K_a^a$, $T = T_a^a$. Integration of Eq. (2.4) over an infinitesimal range along n^a yields

$$K_{ab}^+ - K_{ab}^- = 8\pi G\left(S_{ab} - \frac{1}{2}h_{ab}S\right), \tag{2.5}$$

where the suffix ''+'' denotes a quantity evaluated at the outside of the shell and ''−'' at the inside. Using Eq. (2.5) and the Gauss-Codazzi relation $2G_{ab}n^a n^b = -{}^3R + K_{ab}K^{ab} - K^2$, one finds that the following relation holds for a dust-shell:

$$S^{ab}(K_{ab}^+ + K_{ab}^-) = 0. \tag{2.6}$$

Combining Eqs. (2.5) and (2.6) and substituting the expression of the metric and the stress-energy tensor, we obtain

the following equation for the circumferential radius r_i (the ''expansion law'' of the dust shell):

$$\left(\frac{dr_i}{d\tau}\right)^2=\frac{2GM_+(i)}{r_i}+\left[\left(\frac{M_-(i)}{m_s(i)}\right)^2-1\right]+\frac{G^2m_s^2(i)}{4r_i^2}, \tag{2.7}$$

where $M_\pm$ is defined by

$$M_+(i)\equiv\frac{m_i+m_{i+1}}{2}, \tag{2.8}$$

$$M_-(i)\equiv m_{i+1}-m_i, \tag{2.9}$$

and τ is the proper time of the shell. We have also introduced the ''baryonic'' mass $m_s(i)$ given by $m_s(i)=4\pi s_i r_i^2$ where s_i is the surface density of the ith shell; $s_i=-S^a_a(i)$. It can be shown that this baryonic mass is a constant of motion by the conservation law, $S^b_{a;b}=0$, where the semicolon denotes the three-dimensional covariant derivative on the trajectory of the shell.

In this paper, we shall use a common proper time τ for all the shells. The relation between τ and the time coordinate, t, in Schwarzschild space-time is obtained as follows. First, note that two Schwarzschild time coordinates are assigned to each shell: the ith shell has the time $t_{(-)i}$ measured in the ith region and $t_{(+)i}$ measured in the $(i+1)$th region. Then, from the normalization condition for the 4-velocity of a shell, we obtain

$$\frac{dt_{(+)i}}{d\tau}=\left(\frac{r_i}{r_i-2Gm_{i+1}}\right)\left[1-\frac{2Gm_{i+1}}{r_i}+\left(\frac{dr_i}{d\tau}\right)^2\right]^{1/2}, \tag{2.10}$$

$$\frac{dt_{(-)i}}{d\tau}=\left(\frac{r_i}{r_i-2Gm_i}\right)\left[1-\frac{2Gm_i}{r_i}+\left(\frac{dr_i}{d\tau}\right)^2\right]^{1/2}. \tag{2.11}$$

The procedure to determine the initial points of each time coordinate is described later.

B. The solution and initial condition

In order to specify a dust-shell universe, we have to fix the parameters in Eq. (2.7) and the initial hypersurface. We first rewrite Eq. (2.7) in the form corresponding to the Hubble equation of FL models. We denote the initial circumferential radius of the ith shell by x_i, i.e.,

$$r_i=x_i \quad \text{on initial hypersurface.} \tag{2.12}$$

We define ρ_i by

$$M_+(i)\equiv\frac{4}{3}\pi\rho_i x_i^3, \tag{2.13}$$

and k_i by

$$\left(\frac{M_-(i)}{m_s(i)}\right)^2\equiv 1-k_i x_i^2. \tag{2.14}$$

Then the expansion law of the dust-shell is written as

$$\left(\frac{1}{r_i}\frac{dr_i}{d\tau}\right)^2=\frac{8}{3}\pi G\rho_i\left(\frac{x_i}{r_i}\right)^3-k_i\left(\frac{x_i}{r_i}\right)^2+\frac{G^2m_s^2(i)}{4r_i^4}. \tag{2.15}$$

We see that the first term behaves like a non-relativistic matter term in the Hubble equation of FL models, the second and the third like a curvature and a radiation source term. From this point of view, ρ_i and k_i play roles of the ''energy density'' and the ''curvature,'' respectively. The radiation-like term might be regarded as the effect of the binding energy of the shell [14]. Further, it is worthwhile to note that this radiation-like term is consistent with Futamase's result about the effect of the small-scale inhomogeneities on the global cosmic expansion [4]. Seeing this, one may expect that the inhomogeneities tend to make the Hubble parameter larger compared with a homogeneous universe which has the same ''energy density'' of non-relativistic matter. However, this radiation-like term does not necessarily imply the larger Hubble parameter. In order to see the effect of this term on the Hubble parameter, we need to investigate the distance-redshift relation by solving the null geodesic equations and compare the result in the inhomogeneous space-time and that of the FL model. Such an analysis will be performed in the following sections.

A dust-shell universe is specified if we set the parameters contained in Eq. (2.15), i.e., ρ_i, k_i, x_i, and an initial hypersurface. When we increase the number of the shells to infinity with ρ_i and k_i being finite and independent of i (we will mention this limit as ''large N limit''), the dust-shell universe approaches a FL model if we take an appropriate initial hypersurface, as we will see in Sec. III. Then the parameters ρ_i and k_i agree with the ordinary energy density and curvature in the Hubble equation.

We take

$$k_i=0 \tag{2.16}$$

for all i in the remaining sections. This means that the increase in the gravitational mass m_i is equal to the baryonic mass of the shell. In other words, the kinetic energy of the shell balances with the potential energy, and hence the total energy becomes equal to the rest mass. This is also the simplest case which approaches a flat FL model in the large N limit. Choice of the other parameters and the initial hypersurface will be discussed in Sec. III.

For notational convenience, we shall introduce the following quantities:

$$\mu_i\equiv 2Gm_i, \quad \nu_i\equiv\frac{1}{2}Gm_s(i) \quad \text{and} \quad \sigma_i\equiv 2GM_+(i). \tag{2.17}$$

From Eqs. (2.8) and (2.9), the following relations hold:

$$\mu_i=\sigma_i-2\nu_i, \tag{2.18}$$

$$\mu_{i+1}=\sigma_i+2\nu_i. \tag{2.19}$$

Then the equation for the circumferential radius, r_i, of the ith shell is written in the form

$$\frac{dr_i}{d\tau}=\frac{1}{r_i}\sqrt{\sigma_i r_i+\nu_i^2}, \tag{2.20}$$

where we have assumed that each shell initially expands. From Eqs. (2.10) and (2.11), the equations for the Schwarzschild time coordinates, $t_{(\pm)i}$, are obtained as

$$\frac{dt_{(\pm)i}}{d\tau}=\frac{r_i\mp\nu_i}{r_i-\sigma_i\mp 2\nu_i}. \tag{2.21}$$

Thus, from Eqs. (2.20) and (2.21), the equations for the relations between $t_{(\pm)i}$ and r_i are given by

$$\frac{dt_{(\pm)i}}{dr_i}=\frac{r_i(r_i\mp\nu_i)}{(r_i-\sigma_i\mp 2\nu_i)\sqrt{\sigma_i r_i+\nu_i^2}}. \tag{2.22}$$

The above equations can be integrated easily to give the solution for $r_i>\sigma_i\pm 2\nu_i$ in the form

$$t_{(\pm)i}(r_i)=(\sigma_i\pm 2\nu_i)\ln\frac{\sqrt{\sigma_i r_i+\nu_i^2}-(\sigma_i\pm\nu_i)}{\sqrt{\sigma_i r_i+\nu_i^2}+(\sigma_i\pm\nu_i)} + T_{(\pm)i}(r_i)+\mathcal{T}_{(\pm)i}, \tag{2.23}$$

where

$$T_{(\pm)i}(r_i)=\frac{2}{3\sigma_i^2}(\sigma_i r_i+3\sigma_i^2\pm 3\nu_i\sigma_i-2\nu_i^2)\sqrt{\sigma_i r_i+\nu_i^2}, \tag{2.24}$$

and $\mathcal{T}_{(\pm)i}$'s are integration constants.

There is a coordinate singularity on the Killing horizon; $t_{(\pm)i}$ becomes infinite on $r_i=\sigma_i\pm 2\nu_i$. For further calculation the null coordinate is convenient, since we are interested in the null geodesics in this space-time. Hence, we shall adopt the Kruscal null coordinate which has no coordinate singularity. Outside the horizon in the ith region, $r>\mu_i$, the Kruscal null coordinate is given by

$$U\equiv -2\sqrt{2\mu_i}(r-\mu_i)^{1/2}\exp\left(-\frac{t-r}{2\mu_i}\right), \tag{2.25}$$

$$V\equiv +2\sqrt{2\mu_i}(r-\mu_i)^{1/2}\exp\left(+\frac{t+r}{2\mu_i}\right), \tag{2.26}$$

where U and V correspond to the retarded time and the advanced time. Using these Kruscal coordinates, the line element in the ith region is expressed as

$$ds_i^2=-\frac{\mu_i}{2r}\exp\left(-\frac{r}{\mu_i}\right)dUdV+r^2d\Omega^2. \tag{2.27}$$

Similarly to the Schwarzschild time coordinate, two pairs of Kruscal null coordinates, $U_{(\pm)i}$ and $V_{(\pm)i}$, are assigned to each shell. Using Eq. (2.23), we obtain the Kruscal null coordinates labeling the ith shell in the form

$$U_{(\pm)i}(r_i)=-2\sqrt{2}\sqrt{1\pm\frac{2\nu_i}{\sigma_i}}(\sqrt{\sigma_i r_i+\nu_i^2}+\sigma_i\pm\nu_i) \times\exp\left(\frac{r_i-T_{(\pm)i}-\mathcal{T}_{(\pm)i}}{2(\sigma_i\pm 2\nu_i)}\right), \tag{2.28}$$

$$V_{(\pm)i}(r_i)=+2\sqrt{2}\sqrt{1\pm\frac{2\nu_i}{\sigma_i}}(\sqrt{\sigma_i r_i+\nu_i^2}-\sigma_i\mp\nu_i) \times\exp\left(\frac{r_i+T_{(\pm)i}+\mathcal{T}_{(\pm)i}}{2(\sigma_i\pm 2\nu_i)}\right). \tag{2.29}$$

As expected, $U_{(\pm)i}$ and $V_{(\pm)i}$ are finite on $r_i=\sigma_i\pm 2\nu_i$ and are well defined also for $r_i<\sigma_i\pm 2\nu_i$. When $\sigma_i\pm 2\nu_i$ is larger than r_i, both $U_{(\pm)i}$ and $V_{(\pm)i}$ are negative. This means that the ith shell with $r_i<\sigma_i\pm 2\nu_i$ is located in the white hole part of the Schwarzschild space-time. This situation occurs for the shells beyond the horizon scale.

The determination of the integration constants $\mathcal{T}_{(\pm)i}$ corresponds to the choice of the initial hypersurface. The procedure to construct the initial hypersurface we adopt is summarized as follows; first, we choose a unit spacelike vector $\mathscr{E}^a$ which is directed outward in the ordinary sense with respect to r. Taking this vector as a starting tangential vector, we extend a spacelike geodesic curve until it reaches the second shell. This spacelike geodesic curve defines the simultaneous hypersurface in the region between the first shell and the second shell. Next we extend from this intersection towards the third shell another spacelike geodesic which starts from another spacelike vector at the second shell. This second spacelike geodesic generates a spacelike hypersurface in this region. Repeating this process, we complete the whole initial hypersurface.

From the above procedure, the integration constant of Eq. (2.23) is determined as follows. In the ith region, the tangent vector of the spacelike geodesic is written as

$$\mathscr{E}^t=E_i\left(1-\frac{\mu_i}{r}\right)^{-1} \quad\text{and}\quad \mathscr{E}^r=\sqrt{1+E_i^2-\frac{\mu_i}{r}}, \tag{2.30}$$

and the other components vanish, where E_i is an integration constant associated with the geodesic equation and will be determined by the condition which we will see in the next section. From Eq. (2.30), the equation for the trajectory of the spacelike geodesic in the (t,r) plane is given by

$$\frac{dt}{dr}=\frac{E_i r^{3/2}}{(r-\mu_i)\sqrt{(1+E_i^2)r-\mu_i}}. \tag{2.31}$$

Integrating the above equation, we obtain

$$t=F_i(r)+D_i, \tag{2.32}$$

where

$$F_i(r)=\frac{E_i\sqrt{r}\sqrt{(1+E_i^2)r-\mu_i}}{1+E_i^2}+\mu_i\ln\left(\frac{\sqrt{(1+E_i^2)r-\mu_i}-E_i\sqrt{r}}{\sqrt{(1+E_i^2)r-\mu_i}+E_i\sqrt{r}}\right)+\frac{E_i(3+2E_i^2)\mu_i\ln(\sqrt{(1+E_i^2)r-\mu_i}+\sqrt{(1+E_i^2)r})}{(1+E_i^2)^{3/2}},\tag{2.33}$$

and D_i is an integration constant. Initially, we set $t_{(+)i}=t_{(-)i}$ and $t_{(\pm)1}=0$. Then, since $t_{(-)i-1}=F_{i-1}(x_{i-1})+D_{i-1}$ and $t_{(+)i-1}=F_i(x_{i-1})+D_i$, we find

$$D_i=D_{i-1}+F_{i-1}(x_{i-1})-F_i(x_{i-1}),\tag{2.34}$$

and $D_1=-F_1(x_1)$. From the above recurrent relation, we obtain

$$D_i=-F_i(x_{i-1})+\sum_{j=2}^{i-1}[F_j(x_j)-F_j(x_{j-1})].\tag{2.35}$$

Using these relations, we obtain the integration constants, $\mathcal{T}_{(\pm)i}$, for $i\geqslant 2$ as

$$\mathcal{T}_{(\pm)i}=\sum_{j=2}^{i}[F_j(x_j)-F_j(x_{j-1})]-(\sigma_i\pm 2\nu_i)\times\ln\frac{\sqrt{\sigma_i x_i+\nu_i^2}-(\sigma_i\pm\nu_i)}{\sqrt{\sigma_i x_i+\nu_i^2}+(\sigma_i\pm\nu_i)}-T_{(\pm)i}(x_i),\tag{2.36}$$

and for $i=1$ as

$$\mathcal{T}_{(\pm)1}=-(\sigma_1\pm 2\nu_1)\ln\frac{\sqrt{\sigma_1 x_1+\nu_1^2}-(\sigma_1\pm\nu_1)}{\sqrt{\sigma_1 x_1+\nu_1^2}+(\sigma_1\pm\nu_1)}-T_{(\pm)1}(x_1).\tag{2.37}$$

C. Redshift and diameter distance

We consider a light ray which is emitted from each shell toward an observer at the center. The light ray goes along a future directed ingoing radial null geodesic, where ''ingoing'' refers to the direction from a shell toward shells labeled by a smaller number.

An ingoing radial null geodesic is specified by a constant V in the Kruscal null coordinate. The circumferential radius of the ith shell when it intersects the null geodesic is denoted by R_i. The outermost shell considered here is labeled by M. Then $R_M=x_M$ and hence in the Mth region, $V=V_{(-)M}(x_M)$ is satisfied along the null geodesic. Thus, on the $(M-1)$th shell, the following relation holds

$$V_{(+)M-1}(R_{M-1})=V_{(-)M}(x_M).\tag{2.38}$$

This equation determines R_{M-1}. We obtain the circumferential radii of all the shells at the intersection with the null geodesic by the same procedure, i.e., by solving the following recurrent relation:

$$V_{(+)i}(R_i)=V_{(-)i+1}(R_{i+1}).\tag{2.39}$$

We can determine R_i from the given R_{i+1} through this equation.

In order to derive the expression of redshift, we first write down the components of the null geodesic tangent in the ith region, $k^\mu(i)$, which is given in the Kruscal null coordinate as

$$k^U(i)=\frac{2r}{\mu_i}\exp\left(\frac{r}{\mu_i}\right)\omega_i,\tag{2.40}$$

and the other components vanish, where ω_i is an integration constant associated with the geodesic equation. We require that the observed frequency of the photon at each shell is uniquely determined. The observed frequency, $\omega_{\rm ob}(i)$, at the ith shell is given by

$$\omega_{\rm ob}(i)=-k_\mu(i)u^\mu_{(+)}(i)=\frac{1}{2}\omega_i\frac{dV_{(+)i}}{d\tau},\tag{2.41}$$

$$\omega_{\rm ob}(i+1)=-k_\mu(i)u^\mu_{(-)}(i+1)=\frac{1}{2}\omega_i\frac{dV_{(-)i+1}}{d\tau},\tag{2.42}$$

where

$$\frac{dV_{(\pm)i}}{d\tau}=\frac{\sqrt{2}(\sqrt{\sigma_i R_i+\nu_i^2}\mp\nu_i)}{\sqrt{\sigma_i^2\pm 2\nu_i\sigma_i}}\times\exp\left(\frac{R_i+T_{(\pm)i}(R_i)+\mathcal{T}_{(\pm)i}}{2(\sigma_i\pm 2\nu_i)}\right).\tag{2.43}$$

Equations (2.41) and (2.42) give the relation between $\omega_{\rm ob}(i)$ and $\omega_{\rm ob}(i-1)$, for $i\geqslant 2$, as

$$\omega_{\rm ob}(i)=f(i)\omega_{\rm ob}(i-1),\tag{2.44}$$

where

$$f(i)\equiv\frac{dV_{(-)i}/d\tau}{dV_{(+)i-1}/d\tau}.\tag{2.45}$$

For the first region, a direct calculation leads to

$$\omega_{\rm ob}(1)=\frac{\omega_{\rm ob}(0)}{R_1}(R_1+\nu_1+\sqrt{\sigma_1 R_1+\nu_1^2})\equiv f(1)\omega_{\rm ob}(0),\tag{2.46}$$

where $\omega_{\rm ob}(0)$ is the frequency of the light ray observed by an observer rest at the origin $r=0$. Thus, using the above

relations, we obtain the redshift of the light ray emitted from the ith shell toward the observer rest at $r=0$ in the form

$$1+z(i)=\frac{\omega_{\rm ob}(i)}{\omega_{\rm ob}(0)}=\prod_{j=1}^{i} f(j). \tag{2.47}$$

Our next task is to find the angular diameter-distance $d_{\rm A}$. The definition of $d_{\rm A}$ is

$$d_{\rm A}\equiv\frac{D}{\theta} \tag{2.48}$$

where D is the physical length of the source perpendicular to the line of sight, and θ is the observed angular size. Since the space we are considering is spherically symmetric, the diameter distance from the observer at the center to the ith shell agrees with the circumferential radius R_i when the null geodesic intersects it;

$$d_{\rm A}(i)=R_i. \tag{2.49}$$

We calculate the $d_{\rm A}$-z relation in the dust-shell universe using the relations (2.39), (2.47) and (2.49).

III. RESULTS AND DISCUSSION

A. Setting the parameters of dust-shell model

As mentioned in the previous section, the choice of the parameters and the initial hypersurface determines the behavior of a dust-shell universe. Since we are interested in cases which have a FL limit, we set the parameters so that they approach a FL model in the large N limit.

For most cases described below, we set the mass distribution of shells as

$$\rho_i=\rho_{\rm c}\ \ (\text{independent of}\ \ i), \tag{3.1}$$

at the initial slice. This is not unique, but the simplest case which goes to a FL model in the large N limit. Using $\rho_{\rm c}$, we define $H_{\rm shell}$ and $r_{\rm H}$ by

$$H_{\rm shell}^2\equiv r_{\rm H}^{-2}\equiv\frac{8\pi G}{3}\rho_{\rm c}. \tag{3.2}$$

In terms of FL models, $H_{\rm shell}$ and $r_{\rm H}$ may be regarded as the ''Hubble constant'' and ''Hubble horizon radius.'' However, we cannot say anything at this stage about what relation they have with the Hubble constant and horizon scale of FL models.

For x_i, we put

$$x_i(\tau_{\rm init})=i\Delta x \tag{3.3}$$

with a constant interval Δx

$$\Delta x\equiv\frac{r_{\rm H}}{N_{\rm H}} \tag{3.4}$$

where $N_{\rm H}$ is some positive integer. Here note that $x_{N_{\rm H}}=r_{\rm H}$ and the following relation holds

$$\frac{2GM_+(N_{\rm H})}{x_{N_{\rm H}}}=1. \tag{3.5}$$

Hence $r_{\rm H}$ corresponds to the ''mean Schwarzschild radius'' of the $N_{\rm H}$th and $(N_{\rm H}+1)$th regions.

Before we proceed, we estimate the magnitude of the radiation-like term in equation (2.15). From Eqs. (2.13) and (2.8) with $m_1=0$, we find

$$Gm_{2n-1}=\frac{1}{N_{\rm H}^3}(n-1)^2(4n-1)r_{\rm H}, \tag{3.6}$$

$$Gm_{2n}=\frac{1}{N_{\rm H}^3}n^2(4n-3)r_{\rm H}, \tag{3.7}$$

where n is a positive integer. From Eqs. (2.16), (2.14), and (2.9), we find $m_{\rm s}(i)=m_{i+1}-m_i$ and obtain

$$Gm_{\rm s}(2n-1)=\frac{6n^2-6n+1}{N_{\rm H}^3}r_{\rm H}, \tag{3.8}$$

$$Gm_{\rm s}(2n)=\frac{6n^2}{N_{\rm H}^3}r_{\rm H}. \tag{3.9}$$

Thus, when we consider a large N limit with fixing $x_i=r_{\rm H}(i/N_{\rm H})$, the baryonic mass $Gm_{\rm s}(i)=\mathcal{O}(N_{\rm H}^{-1})$ is regarded as a small quantity, compared with $GM_+(i)$ and Gm_i. That is, the radiation-like term is of order $N_{\rm H}^{-2}$ of the first term and can be neglected when $N_{\rm H}$ is large.

B. Distance-redshift relation in ''orthogonal'' model

As described in the previous section, the choice of E_i corresponds to choice of initial hypersurface. In a FL model, the simultaneous hypersurface is orthogonal to the trajectory of matter. Thus, we try choosing E_i so that the vector ℓ^a is orthogonal to the trajectory of each shell (we will refer to this choice as ''model A''). From the condition $\ell_a u^a_{(+)}(i-1)=0$ at $r=r_{i-1}$, we obtain

$$E_i=\frac{1}{r_{i-1}}\sqrt{\sigma_{i-1}r_{i-1}+\nu_{i-1}^2}. \tag{3.10}$$

In Fig. 2 we plot the angular diameter distance as a function of redshift of each shell for various $N_{\rm H}$ with a common $H_{\rm shell}$ in the case of model A. The total number of shells $N_{\rm T}$ is taken to be $3N_{\rm H}$. We emit a photon toward the center from each shell so that every photon reaches the center si-

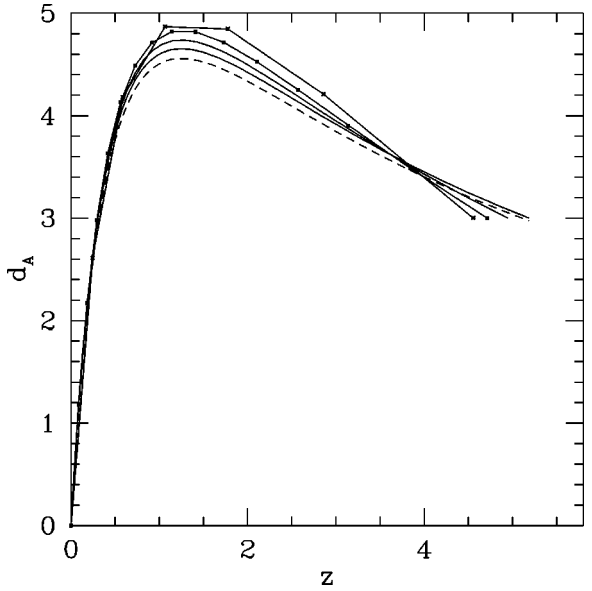

FIG. 2. Angular diameter distance-redshift relation in dust-shell universe for model A. Data points are connected by solid lines. The definition of the models is summarized at the end of Sec. III. The number of shells within the initial Hubble horizon N_H is 2, 5, 10, and 50 from top to bottom around the maximum. The total number of shells N_T is taken to be $3N_H$. We also mark the data by dots in the cases $N_H=2$ and 5. We see that all the curves are quite similar; the deviation among the curves is at most about 10%. On the other hand, it can be also seen that the slope at higher redshifts becomes steeper as we decrease the number of shells. The dashed line shows the d_A-z relation in the flat FL model with $H_i=H_{shell}$. The redshift of the initial hypersurface is identified with the redshift of the outermost shell for the case $N_T=150$, i.e., $z_i=z$ $(i=150)$. The deviation between the flat FL model and the dust-shell universe with $N_T=150$ amounts to about 2% around the maximum of the curve.

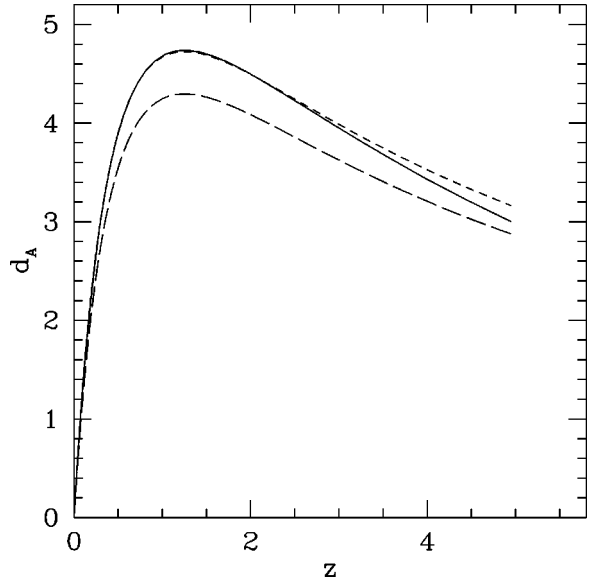

FIG. 3. Angular diameter distance-redshift relation in the dust-shell universe for model A in the case of $N_H=10$ (solid line) and that in the flat FL model with $H_i=H_{shell}$ and $z_i=z$ $(i=30)$ (long dashed line). We see that the deviation among them amounts to about 10%. To see the difference in the shape of the curve, we also plotted a FL curve with a Hubble parameter changed by 10%: $H_i=H_{shell}\times 0.9$ (short dashed line). We see that the slope at higher redshifts is steeper in the dust-shell universe than in the FL model.

multaneously. We have obtained a surprising result that all the curves are quite similar even in the case when we put only two shells within the initial horizon radius; the deviation among the curves is at most about 10%. On the other hand, it can be also seen that the slope at higher redshifts becomes steeper as we decrease the number of shells.

We compare the d_A-z relation in the dust-shell universe obtained above with that of a FL model. We here adopt a spatially flat FL model, since the ''curvature'' term in the expansion law of a dust-shell (2.15) vanishes. Moreover, when N_H is large, the ''radiation'' term is negligible compared to the first term. Thus, in this paper, we focus on the cases with large $N_H(\geqslant 10)$, and compare them with a spatially flat FL model filled only with non-relativistic matter. The cases with small $N_H(<10)$ will be mentioned later.

The Hubble equation in this flat FL model is

$$H^2\equiv\left(\frac{\dot{a}}{a}\right)^2=\frac{8}{3}\pi G\rho_{FL} \tag{3.11}$$

with $\rho_{FL}\propto a^{-3}$. The relation between the redshift and the scale factor in FL models is $1+z=a_0/a$ where subscript ''0'' denotes a value when the observer receives the photon. Thus we can write the present Hubble parameter H_0 in terms of the initial Hubble parameter H_i and redshift z_i as

$$H_0^2=H_i^2(1+z_i)^{-3}. \tag{3.12}$$

The d_A-z relation in the flat FL model is calculated once we fix H_i and z_i, since the relation is determined solely by H_0.

The dashed line in Fig. 2 shows the d_A-z relation in the flat FL model with $H_i=H_{shell}$. The redshift of the initial hypersurface is identified with the redshift of the outermost shell for the case $N_T=3N_H=150$, i.e., $z_i=z(i=150)$. The deviation of the dust-shell universe from the flat FL model with $N_T=150$ amounts to about 2% around the maximum of the curve. We have confirmed that the deviation from the FL model becomes small as we increase N_H. For smaller N_H, however, the redshift of the outermost shell becomes small, resulting in a larger H_0 from the relation (3.12). We show in Fig. 3 the d_A-z relation in the dust-shell universe in the case of $N_H=10$ (solid line) and that in the flat FL model with $H_i=H_{shell}$ and $z_i=z$ $(i=30)$ (long dashed line). In this case, the deviation amounts to about 10%. Moreover, the difference lies not only in the normalization of H_0, but also in the shape of the curve. To see this, we also plotted a FL curve (short dashed line) with a Hubble parameter changed by 10%: $H_i=0.9\times H_{shell}$. Note that the change in the Hubble parameter of the FL model only results in the change in the normalization of the curve. We see that the slope at higher

redshifts is steeper in the dust-shell universe than in the FL model. It is also clear from Fig. 2 that this tendency becomes strong as we decrease $N_{\rm H}$.

Thus, we can say that for large $N_{\rm H}$, the flat FL model approximates the dust-shell universe quite well, but as we decrease N_H, this fit becomes poorer.

In the next subsection we discuss the reason for this behavior by studying the behavior of averaged density, and try to reduce the deviation from FL models without increasing $N_{\rm H}$.

C. Behavior of averaged density

We usually regard a FL model as a large-scale ''average'' of a locally inhomogeneous universe. We will study the relation between the results obtained in the previous section and an ''averaged'' density of the dust-shell universe. We consider an averaged density around the observer at the center. The averaged density is defined by dividing the mass contained within some radius by the 3-volume on the hypersurface up to that radius. We will study the behavior of the averaged density when the radius to take the average is gradually increased, and discuss its relation with the distance-redshift relation.

First let us consider the 3-volume on the initial hypersurface defined in the previous section. From Eq. (2.30), the intrinsic metric of the initial hypersurface is given by

$$d\ell_i^2=\frac{r}{(1+E_i^2)r-\mu_i}dr^2+r^2d\Omega^2. \tag{3.13}$$

Using the above line element, we obtain the spatial volume, Vol(i), of the ith region $(i>1)$ on the initial slice in the form

$$\begin{aligned}\mathrm{Vol}(i)&=4\pi\int_{r_{i-1}}^{r_i}\frac{r^{5/2}}{\sqrt{(1+E_i^2)r-\mu_i}}dr\\&=4\pi\left[\sqrt{(1+E_i^2)r-\mu_i}\left(\frac{r^{5/2}}{3(1+E_i^2)}+\frac{5r^{3/2}\mu_i}{12(1+E_i^2)^2}+\frac{5\sqrt{r}\mu_i^2}{8(1+E_i^2)^3}\right)\right]_{r_{i-1}}^{r_i}\end{aligned} \tag{3.14}$$

$$+\frac{5\pi\mu_i^3}{2(1+E_i^2)^{7/2}}\ln\left(\frac{\sqrt{(1+E_i^2)r_i-\mu_i}+\sqrt{(1+E_i^2)r_i}}{\sqrt{(1+E_i^2)r_{i-1}}-\mu_i+\sqrt{(1+E_i^2)r_{i-1}}}\right). \tag{3.15}$$

For $i=1$, Vol(1) is equal to $4\pi r_1^3/3$.

Using this volume, we define the averaged density $\overline{\rho}(i)$ as follows. We sum the baryonic masses up to the $(i-1)$th shell and half of the ith shell, and divided the sum by the 3-volume inside the ith shell:

$$\overline{\rho}(i)\equiv\left\{m_{\rm s}(i)/2+\sum_{j\leqslant i-1}m_{\rm s}(j)\right\}\Big/\sum_{k\leqslant i}\mathrm{Vol}(k). \tag{3.16}$$

It seems natural to take this sum of masses in averaging, since the motion of the ith shell is approximately determined by the sum of the gravitational mass inside the shell [which agrees with the sum of baryonic masses up to $(i-1)$th shell] and half of its baryonic mass; the numerator in the above definition is the same with $M_+(i)$ which appears in the first term in the expansion law (2.7). We plotted in Fig. 4 the averaged density $\overline{\rho}(i)$ for the model described in the previous section. As expected, $\overline{\rho}(i)$ is almost constant near $\rho_{\rm c}$, which may explain the reason the deviation of $d_{\rm A}$-z relation in the dust-shell models from the FL curves is small.

However, the averaged density becomes slightly smaller at the outside region than $\rho_{\rm c}$ defined by the expansion law. The reason is explained as follows. The volume, V, between r_i and $r_{i+1}\equiv r_i+\Delta r$ is expanded in terms of Δr as

$$\begin{aligned}V&=4\pi\int_{r_i}^{r_i+\Delta r}\{l^r(r)\}^{-1}r^2dr=4\pi\int_{r_i}^{r_i+\Delta r}\{l^r(r_i)\}^{-1}r^2dr\\&\quad-4\pi\int_{r_i}^{r_i+\Delta r}l^r(r_i)'\{l^r(r_i)\}^{-2}(r-r_i)r^2dr+\cdots,\end{aligned} \tag{3.17}$$

where $l^{r\prime}=dl^r/dr$. Substituting the expression of l^r, we can expand V in terms of $1/N_{\rm H}$ to find

$$V=4\pi r_i^2\Delta r\left(1+\frac{1}{2}\frac{i}{N_{\rm H}{}^2}+\cdots\right). \tag{3.18}$$

We see that the volume becomes larger than that of a homogeneous model. This effect is significant especially when $i>N_{\rm H}$, i.e., beyond the horizon scale, which explains the behavior of the averaged density at large i in Fig. 4. From this figure, one may think we can reduce the deviation from the FL model by adjusting the expansion law so that the averaged density is a constant value. We plotted the $d_{\rm A}$-z relation in this case (model B) and the corresponding FL curve for

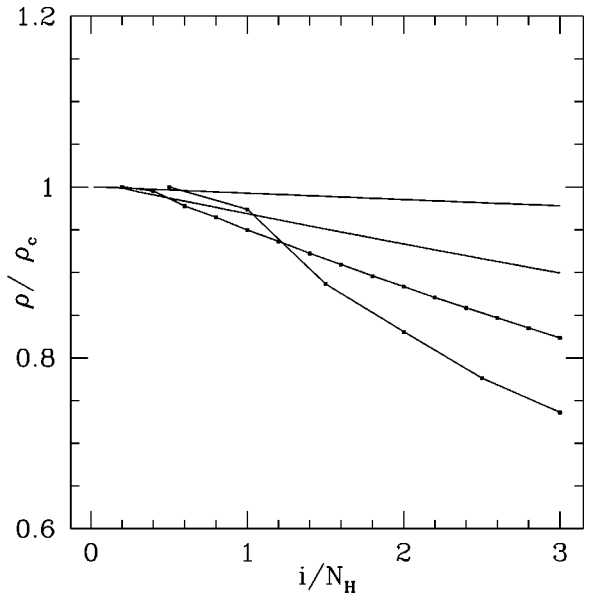

FIG. 4. Averaged density $\overline{\rho}$ normalized by ρ_c in the cases $N_H=2$, 5, 10, and 50 for model A. We connect the data by solid lines. We also mark the data by dots in the cases $N_H=2$ and 5. The curve which is smaller at large i corresponds to the curve with smaller N_H. We see that the averaged density $\overline{\rho}(i)$ is almost constant near ρ_c, especially for small i, which may explain that the deviation of d_A-z relation in the dust-shell models from the FL curves is small. One also notices that the averaged density becomes smaller at the outside region than ρ_c. The interpretation of this behavior is discussed in the text.

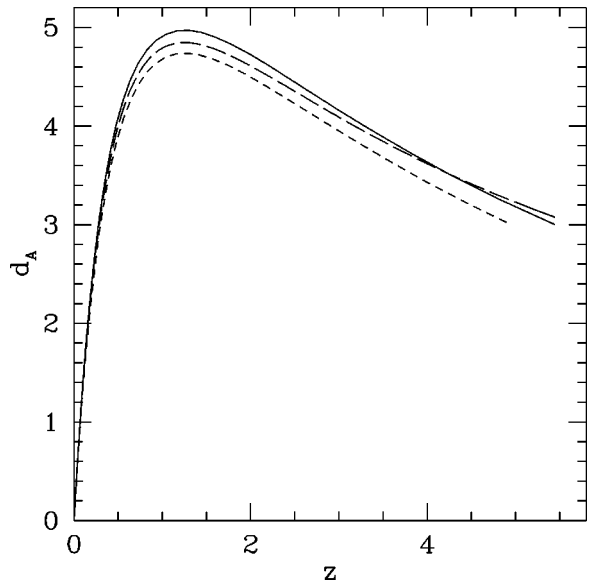

FIG. 5. Angular diameter distance-redshift relation in the dust-shell universe for model B in the case of $N_H=10$ (solid line) and that in the flat FL model with $H_i=H_{shell}$ and $z_i=z$ $(i=30)$ (long dashed line). For comparison, we also showed the curve in the dust-shell universe for model A (short dashed line). We see that the difference in the normalization between the dust-shell universe and the FL model is reduced, but the difference in the shape of the curve is not reduced compared with Fig. 3.

$N_H=10$ in Fig. 5 (the solid line and the long dashed line). We adjust ρ_i in the expansion law iteratively so that the relation

$$\overline{\rho}(i)=\frac{3}{8\pi}H_{\rm shell}^2 \tag{3.19}$$

is satisfied. As a result, ρ_i is not homogeneous; it increases as i increases (Fig. 6). From Fig. 5, we see that the difference between the dust-shell universe and the FL model remains the same as Fig. 3, although the averaged density is indeed a constant.

D. Cases with homogeneous averaged density field

We can take an initial hypersurface in which both ρ_i and $\overline{\rho}(i)$ is homogeneous by requiring the relation

$$\mathrm{Vol}(i)=\frac{4\pi}{3}(r_i^3-r_{i-1}^3). \tag{3.20}$$

We plot the d_A-z relation of this model (model C) in Fig. 7. Comparing with Fig. 2, we see that the difference among the curves is reduced. Figure 8 illustrates the good agreement between the d_A-z relations of the dust-shell model and a FL model for the case $N_H=10$.

Here we check whether the assumption of constant interval $\Delta x=r_H/N_H$ is essential or not. We try some patterns of the initial circumferential radius of the shells x_i, for instance,

$$x_{i+1}=x_i+h\times a^i, \tag{3.21}$$

where h and a are some positive constants and $a\neq 1$. When $a>1(<1)$, the distribution of shells becomes sparser (denser) for larger i. We have found that the results are unchanged. We also try another pattern

$$x_{2n}=2n\times\Delta x, \tag{3.22}$$

$$x_{2n+1}=(2n+1)\times\Delta x+a\Delta x, \tag{3.23}$$

with $a\neq 0$. We plotted the result when $N_H=10$, $N_T=30$, and $a=0.05$ (model D) in Fig. 9.[2] We can see that the deviation from the FL model remains small.

We can take another interesting choice; the expansion law is homogeneous (characterized by ρ_c), and the averaged density is also homogeneous, but each quantity differs; $\rho_c=a\overline{\rho}$ (model E). This is realized by imposing a condition of the form

[2]There is a maximum in a according to N_T when we impose the condition $\overline{\rho}(i)=\rho_i=\rho_c$; if we increase N_T, the maximum value allowed for a becomes small. The value of a adopted here is about the maximum value for $N_T=3N_H$.

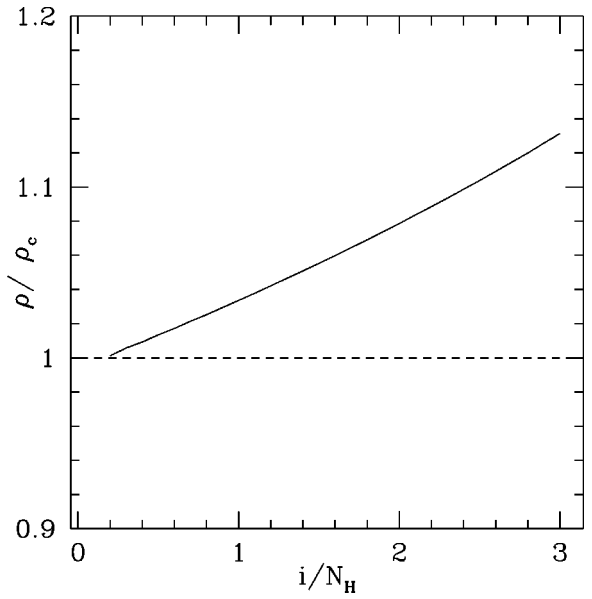

FIG. 6. The averaged density $\overline{\rho}$ (dashed line) and the parameter ρ_i (solid line) which determines the expansion law of the shells of model B. We see that ρ_i increases as i increases, while the averaged density $\overline{\rho}$ is indeed a constant.

$$\mathrm{Vol}(i) = a\frac{4\pi}{3}(r_i^3 - r_{i-1}^3), \tag{3.24}$$

with $a \neq 1$. In Fig. 10, we show the result in the case $N_H = 10$ and $a = 0.93$ (solid line). The dashed lines are curves in a FL model. The upper one uses the original ''Hubble constant'' [Eq. (3.2)], i.e., $H_i = H_{shell}$, and the lower one uses the parameter changed by the same amount with the change in the volume, i.e., $H_i^2 = H_{shell}^2 \times a^{-1}$. We see that the shape of the curve differs from a FL curve (compare with Fig. 8). This indicates that the averaged density should agree with ρ_c which determines the expansion law, in order for the d_A-z relation to behave like that of a FL model. It should be also

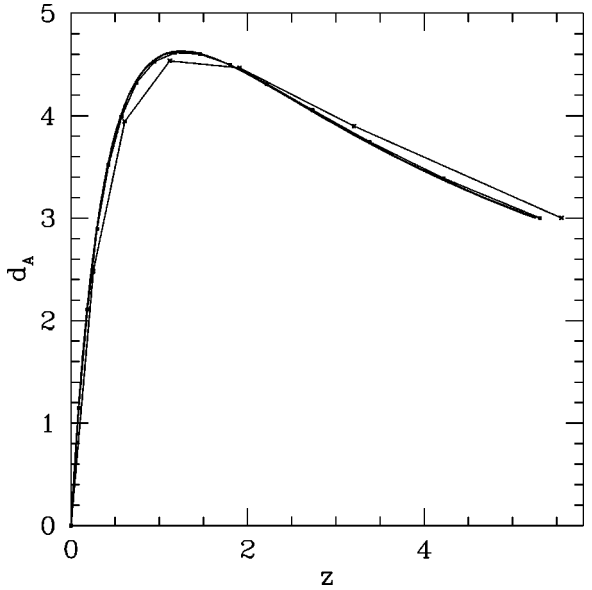

FIG. 7. Angular diameter distance-redshift relation in dust-shell universe for model C. The number of shells within the initial Hubble horizon N_H is 2, 5, 10, and 50. The total number of shells N_T is taken to be $3N_H$. Data points are connected by solid lines. We also mark the data by dots in the cases $N_H = 2$ and 5. Comparing with Fig. 2, we see that the difference among the curves is reduced so that it is hard to distingush the curves for $N_H = 5$, 10, and 50.

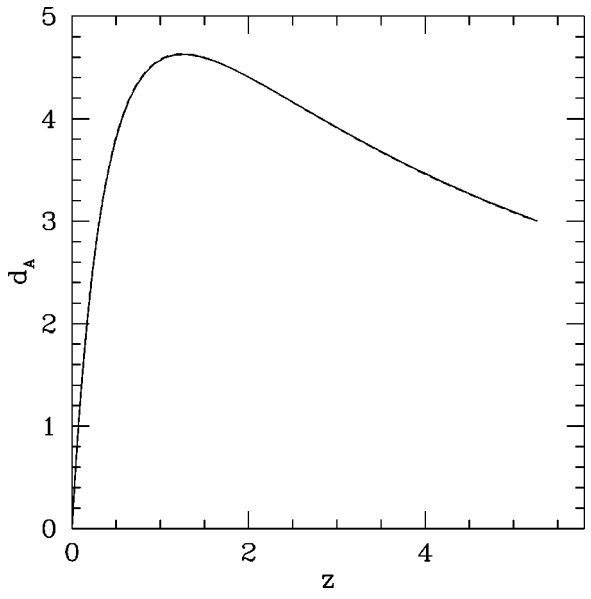

FIG. 8. Angular diameter distance-redshift relation in the dust-shell universe for model C in the case of $N_H = 10$ (solid line) and that in the flat FL model with $H_i = H_{shell}$ and $z_i = z$ ($i = 30$) (dashed line). This illustrates the good agreement between the d_A-z relations of the dust-shell model and of a FL model for the case $N_H = 10$.

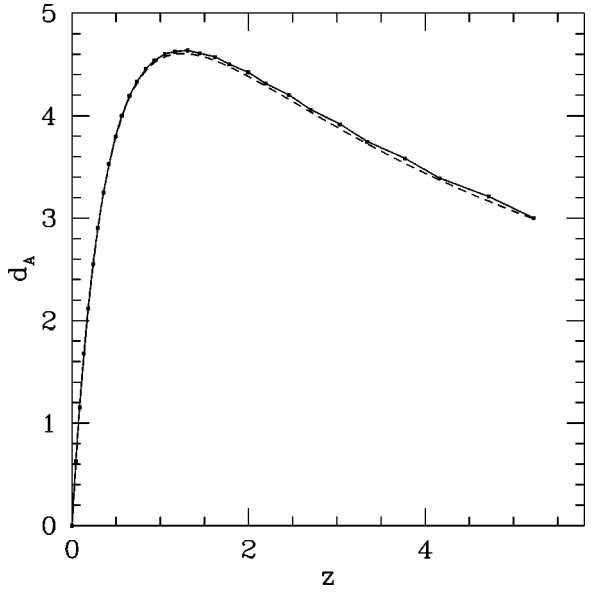

FIG. 9. Angular diameter distance-redshift relation in the dust-shell universe for model D in the case of $N_H = 10$ (solid line and points) and that in the flat FL model with $H_i = H_{shell}$ and $z_i = z$ ($i = 30$) (dashed line). We can see that the deviation from the FL model remains small.

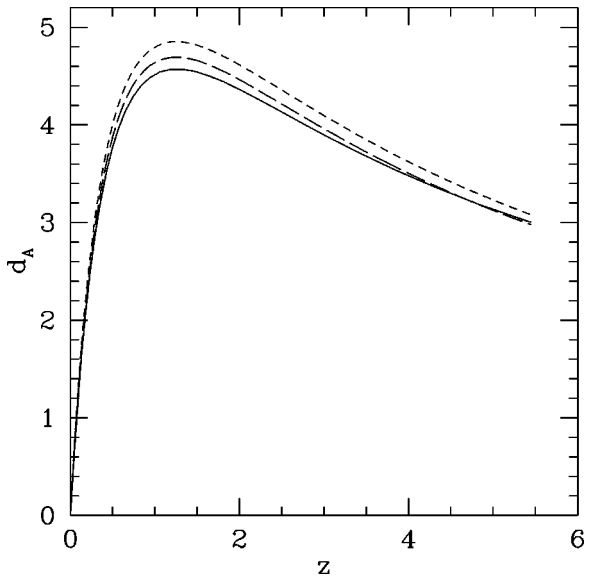

FIG. 10. Angular diameter distance-redshift relation in the dust-shell universe for model E in the case of $N_H=10$ (solid line) and that in the flat FL model with $H_i=H_{shell}$ and $z_i=z$ $(i=30)$ (short dashed line). The long dashed line is the FL curve with the Hubble parameter changed by the same amount with the change in the volume, i.e., $H_i^2=H_{shell}^2\times a^{-1}$. Comparing with Fig. 8, we see that the shape of the curve differs from a FL curve. This indicates that the averaged density should agree with ρ_c which determines the expansion law, in order for the d_A-z relation to behave like that of a FL model. Also note that the FL curve with the changed Hubble parameter (long dashed line) is closer to the curve in dust-shell universe than the other (short dashed line). The interpretation of this behavior is discussed in the text.

noted that the FL curve with the changed Hubble parameter is closer to the curve in dust-shell universe than the other. This may indicate that the ''observed'' Hubble parameter is closer to the averaged density $\overline{\rho}$, rather than ρ_c which determines the expansion law.

E. Summary of models and conclusions

Here we summarize our results.

Model A: The initial hypersurface is orthogonal to each trajectory of shells and the expansion law is homogeneous; $\rho_i=\rho_c$. The d_A-z relation of the dust-shell universe shows deviation from the FL curve, especially when N_H is small (Figs. 2,3). The averaged density $\overline{\rho}$ is not constant (Fig. 4).

Model B: We adjust ρ_i so that $\overline{\rho}=\rho_c$ is satisfied (Fig. 6) on the same initial hypersurface as Model A. The deviation from the FL curve is not reduced (Fig. 5).

Model C: We choose the initial hypersurface so that the relation $\overline{\rho}(i)=\rho_i=\rho_c$ is satisfied. The d_A-z relation of the dust-shell universe shows good agreement with the FL curve (Figs. 7,8).

Model D: The choice of the initial hypersurface is the same as Model C, but the interval of the shells is not constant [Eqs. (3.22),(3.23)]. The deviation of d_A-z relation of the dust-shell universe from the FL curve remains small (Fig. 9).

Model E: The averaged density $\overline{\rho}(i)$ and the parameter ρ_i are homogeneous, but $\overline{\rho}(i)\neq\rho_i$. The d_A-z relation of the dust-shell universe shows mild deviation from the FL curve (Fig. 10).

From these results, we conclude that the d_A-z relation in a dust-shell universe looks like a flat FL universe, when the expansion law resembles the flat FL model, and the behavior of averaged density field is scale-independent when we increase the scale of averaging, and the averaged density agrees with ρ_c. This statement seems to be valid even in the cases with quite small number of the shells. However, the situation is not so simple. In small N_H cases, the radiation-like term in the expansion law cannot be neglected. One may expect that a FL model with radiation term gives a better fitting to those cases, but we have found this does not work. This implies that we cannot tell the effect of homogeneities just by studying the expansion law. We need more detailed study to this problem, which is left for our future work.

We also note that in spatially flat cases the gravitational mass and the baryonic mass coincide; whether we use the baryonic mass or gravitational mass in defining the averaged density, the result is the same. In cases where those masses are different, we have to be careful in determining the averaged density when we try to construct a FL model which fits a dust-shell universe. In order to clarify which mass we should use to construct a fitting FL model, we have to study non-zero k_i cases, which will also be done in our future paper.

IV. SUMMARY

We have studied the behavior of d_A-z relation in a spherically symmetric dust-shell universe where the mass distribution is discrete. We have compared the relation of dust-shell universe with that of FL models, and discussed the relation with the behavior of averaged density. We have seen that the d_A-z relation observed at the center agrees well with that of a flat FL model if the following conditions are satisfied: (i) the expansion law of the circumferential radius of the shells resembles the Hubble equation of a spatially flat FL model, (ii) the behavior of averaged density around the observer at the center is scale-independent as we increase the scale on which we take the average, and (iii) the averaged density agrees with the energy density of the FL model. We have also seen that the choice of initial hypersurface relates the expansion law to the averaged density.

The effect of discreteness of mass distribution appears in the equation of motion of each dust-shell. This effect becomes smaller as we increase the number density of shell. We conclude the discreteness of matter distribution itself is of no significance in this model in discussing the observed quantities such as d_A and z, as long as the expansion law and the averaged density field is homogeneous in the sense described above. This supports the averaging hypothesis that a universe is described by a FL model if the universe is homogeneous when the density is averaged on some scale larger than the scale of the inhomogeneities.

We need, however, further discussion for the cases when the number of shells is extremely small, and when the cur-

vature term does not vanish. We also note that it will be interesting to study cases where the averaged density is inhomogeneous or non-radial null rays travel, to see cosmological lensing effects. These problems are left for our future work.

ACKNOWLEDGMENTS

We would like to thank H. Sato for encouragement. N.S. and T.H. are supported by Japan Society for the Promotion of Science for Young Scientists Grant Nos. 3167 and 9204.

[1] S. Weinberg, *Gravitation and Cosmology* (Wiley, New York, 1973).
[2] G.F. Smoot *et al.*, Astrophys. J. Lett. **396**, L1 (1992).
[3] G.F.R. Ellis, *in Proceedings of 10th International Conference on General Relativity and Gravitation*, edited by B. Bertotti *et al.* (Reidel, Dordrecht, 1984).
[4] T. Futamase, Phys. Rev. Lett. **61**, 2175 (1988); Mon. Not. R. Astron. Soc. **237**, 187 (1989); Prog. Theor. Phys. **86**, 389 (1991); Phys. Rev. D **53**, 681 (1996).
[5] T. Buchert and J. Ehlers, Astron. Astrophys. **320**, 1 (1997).
[6] H. Russ, M.H. Soffel, M. Kasai, and G. Börner, Phys. Rev. D **56**, 2044 (1997).
[7] M. Carfora and K. Piotrkowska, Phys. Rev. D **52**, 4393 (1995).
[8] M. Kasai (private communication).
[9] S. Bildhauer, Prog. Theor. Phys. **84**, 444 (1990).
[10] S. Bildhauer and T. Futamase, Mon. Not. R. Astron. Soc. **249**, 126 (1991).
[11] R.M. Wald, *General Relativity* (University of Chicago Press, Chicago, 1984).
[12] C.W. Misner, K.S. Thorne, and J.A. Wheeler, *Gravitation* (Freeman, San Francisco, 1973).
[13] W. Israel, Nuovo Cimento B **44**, 1 (1966); *ibid.* **48**, 463 (1967); Phys. Rev. **153**, 1388 (1967).
[14] H. Sato, Prog. Theor. Phys. **76**, 1250 (1986).
[15] K. Maeda, Gen. Relativ. Gravit. **18**, 931 (1986).